Complex macroscopic behavior in systems of phase oscillators with adaptive coupling

Per Sebastian Skardal , Dane Taylor, Juan G. Restrepo

Department of Applied Mathematics, University of Colorado at Boulder, CO 80309, USA

model, which has relatively simple macroscopic dynamics (e.g., no memory). In this paper, we explore the addition of adaptive rules to oscillator systems exhibiting bistability, such as those studied in Refs. [31 34]. When it is combined with adaptation, we find that bistability allows for complex macroscopic behavior such as excitable and intermittently synchronous states in addition to simple steady-state behavior. In this paper, we consider the case where the timescale of coupling adaptation is much larger than the timescale of oscillator dynamics, which will allow us to separate timescales, first solving for the fast oscillator dynamics using the work of Ott and Antonsen [23] and then analyzing the slow adaptation dynamics. We find that even when the adaptation is chosen to be a simple function of the system state, a variety of macroscopic behaviors can be attained by varying parameters of that simple function. The dynamics described in this paper fall within the framework of dynamic bifurcation theory [35], which describes bifurcations that occur in fast dynamics in response to one or more slowly changing parameters. In this paper, the bifurcations correspond to transitions between macroscopic incoherent and synchronized states in response to one or more slowly changing coupling strengths.

This paper is organized as follows. In Section 2, we study a system of time-delayed oscillators subject to uniform adaptation. In Section 3, 3

Fig. 1. (Color online) Solutions R_s (solid blue curve) and R_u (dashed red curve) (given by Eq. (7)) for the time-delayed system with $\omega_0 = 5$, $\tau = 1$, and $\beta = 1$. Inset: Ω_s (solid blue curve) and Ω_u (dashed red curve) corresponding to the angular velocities of the synchronized states. Note that Ω_s and Ω_u are much smaller than the average intrinsic frequency $\omega_0 = 5$ (dotted line).

time-delayed coupling is biased toward oscillators with angular frequencies near Ω. Because Ω is much smaller than ω_0, this distribution of locked frequencies is typically spread asymmetrically around the mean frequency ω_0. We compute the critical frequencies $\omega_{c,\pm}$ separating phase-locked and drifting oscillators by entering a rotating frame in which synchronized oscillators appear stationary by defining $\psi_n = \theta_n - \Omega t$. Here, ψ_n evolves according to $\dot{\psi}_n = \omega_n - \Omega - kR\sin(\psi_n)$, so ψ_n reaches an equilibrium and becomes phase-locked if $|\omega_n - \Omega| \leq kR$, and otherwise drifts indefinitely. Thus, the critical frequencies that separate the drifting and locked populations are $\omega_{c,\pm} = \Omega \pm kR$.

2.2. Slow coupling adaptation

Having solved the oscillator dynamics that evolve on the fast timescale, we now study adaptation given by Eq. (4)
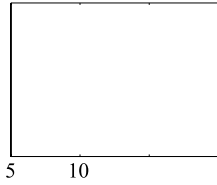
5   10

Fig. 2.   (Color online) Various macroscopic behaviors may occur for uniform adaptation following Eq. (11) depending on   ;   and the location of fixed points (circles). Examples include (a) intermittent, (b) synchronized, (c) ES, and (d) bistable states.

Fig. 3.   (Color online) Bifurcation diagram summarizing boundaries between intermittent, synchronized, ES, incoherent, EI, and bistable states for $\omega_0 = 5$, $\Delta = 1$, and $\Gamma = 1$.

entering the bistable region). In Fig. 3, we show the bifurcation diagram for $\omega_0 = 5$ and $\Delta = 1$ by plotting curves describing the formation/destruction of incoherent fixed points in solid blue, synchronized fixed points in dashed red, and the borders between EI/ES and incoherent/synchronized states in dotted black. We label regions with the states described above. We note that excitable and intermittent states are possible only when $\Gamma < 0$, which we refer to as anti-Hebbian adaptation (accordingly, we refer to $\Gamma > 0$ as Hebbian adaptation). This terminology is based on the observation that, for $\Gamma > 0$ $(\Gamma < 0)$ in Eq. (11), coupling is promoted (inhibited) by the synchrony of oscillators.

2.3. Intermittent case

Motivated by observations of intermittently synchronous dynamics in various applications of oscillator systems (e.g., in neural activity [8,

Fig. 6. (Color online) Example $(\bar{k}, |\bar{r}|)$ trajectories of the system given by Eqs. (19)–(21). The solid blue and dashed red trajectories were obtained using $(\alpha, \beta) = (.24, 0)$ and $(.6, 0)$, respectively, with initial coupling strength $\bar{k} = 6$ and 22, respectively. Other parameters are $\omega_0 = 5; \Delta = 1; \tau = 1; T = 1000; \gamma = 3; d_{min} = 100$, and $N = 1000$.

Fig. 7. (Color online) Bifurcation diagram summarizing oscillatory (black squares), synchronized (red circles), ES (cyan asterisks), incoherent (blue triangles), EI (green plusses), and bistable (yellow crosses) states for network adaptation of time-delayed oscillators with $\tau = 1; \omega_0 = 5; \Delta = 1$, and $T = 1000$.

oscillators, where the degree d is defined as $d_n = \sum_{m=1}^{N} A_{nm}$. The parameters for the oscillator dynamics are $\omega_0 = 5; \Delta = 1; \tau = 1$, and the adaptive timescale is $T = 1000$. The dominant eigenvalue for the network constructed for the simulations shown here is $\lambda_D = 232.325$. In Fig. 6, we show representative $(\bar{k}, |\bar{r}|)$ trajectories. First, using $(\alpha, \beta) = (.24, 0)$, we allow the average coupling strength to increase from an initial value of $\bar{k} = 6$ (solid blue trajectory). Next, using $(\alpha, \beta) = (.6, 0)$, we allow $\bar{k}$ to decrease from an initial value of $\bar{k} = 22$ (dashed red). We find that, in analogy with the uniform adaptation case, a stable synchronized solution $|R| > 0$ is created at $\bar{k} = \bar{k}_1 \approx 12.6$, and the incoherent solution $|R| = 0$ becomes unstable at $\bar{k} = \bar{k}_2 \approx 13.6$. Thus, dynamic bifurcations occur approximately when an incoherent state's average coupling increases through $\bar{k}_2$ or a synchronized state's average coupling decreases through $\bar{k}_1$.

Next, we numerically explore the (α, β) parameter space, classifying the observed behaviors as bistable, intermittent, synchronized, ES, incoherent, and EI, following the criteria in Section 2. In Fig. 7, we plot the results. Starting from the top left and proceeding clockwise, we plot bistable (yellow crosses), synchronized (red circles), ES (cyan asterisks), oscillatory (black squares), EI (green plusses), and incoherent (blue triangles) states. These states were found by tracking the trajectories of $|\bar{r}|$ and $\bar{k}$ for two simulations at each pair (α, β), one trajectory starting from an incoherent state with $\bar{k} < \bar{k}_1$, and the other starting from a synchronized state with
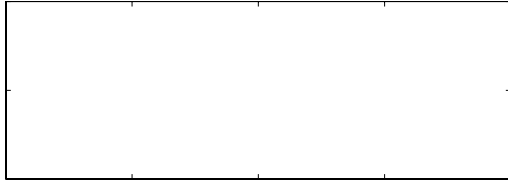
$\bar{k} > \bar{k}_2$. The results are smooth enough that the boundaries between regions are clear. As expected, while the exact boundaries in Fig. 7 differ from those plotted in Fig. 3, the topologies of the two phase spaces agree qualitatively.

3.2. Community interaction

Next, we generalize the system studied in Section 2 to a two-community model in which coupling is strong within communities and weak between communities. For simplicity, we assume that the adaptation within and between each community is uniform. The model we consider is

$$\dot{\theta}_n = \omega_n + \sum_{\sigma=1}^{2} \frac{k_{\sigma}}{N_{\sigma}} \sum_{m=1}^{N_{\sigma}} \sin(\theta_m - \theta_n - \beta)$$

Fig. 8. (Color online) Community interaction model with parameters $\omega_0 = 5$; $\Delta = 1$; $\lambda = 1$; $\gamma = 18$; $\eta = 30$; $T = 200$, and $d = 0.105$ (a) and 0.085 (b). Top panels: evolution of $|r_1|$ (solid blue line) and $|r_2|$ (dashed red line); bottom panels: evolution of k_{11} (solid blue line), k_{22} (dashed red line), k_{12} (dot dashed green line), and k_{21} (dotted black line).

Fig. 9. (Color online) (a) Bifurcation diagram for the Kuramoto model with bimodal frequency distribution. Transcritical, Hopf, homoclinic, and saddle node/SNIPER bifurcations are plotted in dashed back, blue, green, and red, respectively. Paths taken in Fig. 10 are plotted in solid black. (b) Zoomed-in view of bistable regions. We label regions where incoherent, synchronized, and standing-wave solutions are stable In, S, and SW, respectively.

following:

$$\dot{\theta}_n = \omega_n + k \operatorname{Im}(r e^{-i\theta_n}); \tag{29}$$

$$T\dot{k} = G(k; z); \tag{30}$$

where $r = \frac{1}{N} \sum_{n=1}^{N} e^{i\theta_n}$ is the normal Kuramoto order parameter, and now we assume that ω_n are drawn from the double Lorentzian

$$g(\omega) = \frac{\Delta}{2\pi} \left[\frac{1}{(\omega - \omega_0)^2/2 + \Delta^2} + \frac{1}{(\omega + \omega_0)^2/2 + \Delta^2} \right]; \tag{31}$$

which is bimodal for $\Delta < \sqrt{3}\omega_0$. We note that in Ref. [

Fig. 10.   (Color online) $|r.t/|$ versus $k.t/$ trajectories for the Kuramoto model with bimodal frequency distribution with uniform adaptation following Eq. (11) for $N D 2000$ oscillators, $!_0 D 1$; $D 5$; $D 5$; $D 1000$, and $D 0.82$ (a), 0.89 (b), and 1.02 (c). A transition from incoherence to a standing-wave solution in (b) is indicated by an arrow.

4. Discussion

We have investigated analytically and numerically the effect of slow coupling adaptation on models of coupled phase oscillators exhibiting bistability, and have characterized the complex macroscopic behavior that extends to other bistable phase oscillator systems where bistability arises (e.g., due to frequency adaptation [33] or inertial terms [34]). In addition to states with simple macroscopic fixed points, we have observed for uniform coupling adaptation on bistable systems macroscopic excitable and intermittently synchronous states. We leave open the exploration of further dynamics that may occur for systems exhibiting multistability.

Besides considering only uniform coupling adaptation (i.e., allowing the global coupling strength of an all-to-all system to evolve depending on macroscopic system properties), we have also addressed network adaptation (i.e., allowing the links between individual oscillators to evolve according to their local properties). Network adaptation allows for heterogeneities in evolving networks to be accentuated, and it is often more realistic (e.g., Hebbian learning in neural systems [30]). However, we have found that, even when the underlying network structure is heterogeneous, which in turn promotes heterogeneities in the coupling between oscillators, qualitatively similar macroscopic behavior emerges, i.e. fixed points, excitable, and intermittently synchronous states. Although our results for this case are purely numerical, we note that our results from the uniform adaptation model describe more heterogeneous networks with network adaptation very well. The development of more advanced methods for dimension reduction for heterogeneous oscillator networks is an open area of research, although progress continues [43].

We also have considered uniform adaptation for systems with either community interaction or bimodal frequency distributions. In the community interaction model, we have found complicated behavior even for simple parameter assumptions. We hypothesize that changing the manner in which communities interact and/or increasing the number of communities could lead to richer, more complicated dynamics, including chaotic macroscopic states. In the bimodal frequency distribution model, we have demonstrated new dynamic bifurcations corresponding to the transitions between standing-wave solutions and the typical incoherent and synchronized states.

This work also provides a strategy for reconciling the common disconnect between microscopic behavior (i.e. individual oscillator dynamics) and macroscopic phenomena. In the systems studied in this paper, we have shown that entire populations of oscillators can combine into a single functional unit. For example, a wide range of parameters yields intermittent synchronous dynamics, which we liken to clock-like behavior. Similarly, we liken the dynamics of excitable and bistable states to neuron-like firing and switch-like behavior, respectively. One interesting direction of future research motivated by the work presented in this paper is the study of even more complex systems that are composed of many

functional units in a hierarchical organization. In particular, one could study systems built out of different kinds of functional units, for instance to understand the resulting dynamics when networks of clocks, neurons, and switches interact. Because of their analytic when network

[23] E. Ott, T.M. Antonsen, Chaos 18 (2008) 037113.
[24] E. Ott, T.M. Antonsen, Chaos 19 (2009) 023117;
     E. Ott, B.R. Hunt, T.M. Antonsen, Chaos 21 (2011) 025112.
[25] S.A. Marvel, R.E. Mirollo, S.H. Strogatz, Chaos 19 (2009) 043104.
[26] A. Pikovsky, M. Rosenblum, Physica D 240 (2011) 872.
[27] C.B. Saper, T.E. Scammel, J. Lu, Nature 437 (2005) 1257.
[28] B. Rosati, D. McKinnon, Circ. Res. 94 (2004) 874.
[29] Q. Ren, J. Zhao, Phys. Rev. 76 (2007) 016207;
     Y.L. Maistrenko, et al., Phys. Rev. E 75 (2007) 066207;
     M. Li, S. Guan, C.-H. Lai, New J. Phys. 12 (2010) 103032.
[30] P. Seliger, S.C. Young, L.S. Tsimring, Phys. Rev. E 65 (2002) 041906;